Desalination and Water Treatment
www.deswater.com

doi: 10.1080/19443994.2015.1109562

57 (2016) 20076–20083
September

Taylor & Francis
Taylor & Francis Group

Modified poly(vinyl alcohol)-triethylenetetramine nanofiber by glutaraldehyde: preparation and dye removal ability from wastewater

Niyaz Mohammad Mahmoodi*, Zahra Mokhtari-Shourijeh

Department of Environmental Research, Institute for Color Science and Technology, Tehran 1668814811, Iran, Tel. +98 021 22969771; Fax: +98 021 22947537; emails: mahmoodi@icrc.ac.ir, nm_mahmoodi@aut.ac.ir, nm_mahmoodi@yahoo.com (N.M. Mahmoodi), zahramokhtari12885@yahoo.com (Z. Mokhtari-Shourijeh)

Received 27 April 2015; Accepted 29 September 2015

ABSTRACT

In this paper, poly(vinyl alcohol) (PVA)–triethylenetetramine (TETA) nanofiber was prepared and crosslinked using glutaraldehyde (GA). Dye removal ability of the modified nanofiber (PVA–TETA–GA) from colored wastewater was studied. Fourier transform infrared spectroscopy (FTIR) and scanning electron microscopy (SEM) were used to investigate the characteristics of the modified nanofiber. The effect of operational parameters (adsorbent dosage, pH, and the initial dye concentration) on dye removal was studied. The dye adsorption isotherm and kinetics on the nanofiber follows the Langmuir isotherm and pseudo-second-order kinetics, respectively. The results showed that the PVA–TETA–GA nanofiber is a suitable adsorbent with high dye adsorption capacity.

Keywords: Nanofiber; Preparation; Modification; Dye removal; Colored wastewater

1. Introduction

The removal of pollutants from water and wastewater necessitates using the available biological and physicochemical processes including biological, chemical oxidation, photocatalysis, ozonation, precipitation, adsorption, and filtration methods. These methods have been used to remove pollutants including heavy metals, dyes, etc. [1–3].

Adsorption process is the most common method to remove dye from solutions. Several adsorbents such as activated carbon, oxide minerals, polymers, resins, and biomaterials (such as chitosan), have been used to remove dye. Chitosan is the N-deacetylated derivative of chitin and has unique properties such as being non-toxic, having biological degradability and adaptation to nature [4–5]. The adsorption efficiency of adsorbents depends on their properties and surface functional groups. Different surface functional groups including carboxyl, amino, sulfonic, and phosphoric groups have been investigated. Amino group is attractive functional group due to high activity to form strong complexes with pollutants by its nitrogen atom [6].

The electrospinning process has received a lot of attention to prepare nanofiber due to its simplicity and cost-effectiveness. In addition electrospinning is a decades-old technique that draws very fine fibers from a viscous liquid under the force of an electrostatic field. The resulting fibers with high surface area to volume ratio are potential candidates for a variety of fields such as membrane technology [7–10], drug delivery systems, enzyme immobilization, electronics, and sensors. Poly (vinyl alcohol) (PVA) can be used as the organic phase of the hybrid fibers. The biocompatibility, process

*Corresponding author.

ability, and hydrophilicity of PVA have led to its industrial use in areas such as membranes, paints, and adhesives. However, water solubility of PVA limits its use in applications such as ultrafiltration, catalyst support, or biomedical engineering, which require stability in aqueous systems. Thus several researches crosslink PVA to reduce its water solubility using different agents [11–13]. Different chemicals, such as hexamethylene diisocyante, glutaraldehyde and maleic acid, were used as cross-linkers to bind the terminal hydroxyl groups of PVA. Therefore, PVA composite with reduced water solubility should be developed through a cost-effective approach [14–16]. PVA/ZnO nanofiber was used to remove metal ions from aqueous solution. The equilibrium data showed that the capacity values of 370.86, 162.48, and 94.43 mg/g for the sorption of U (VI), Cu(II), and Ni(II) ions, respectively, were obtained at contact time 6 h, temperature 45˚C, adsorbent concentration 1 g/L and pH 5 [17].

A literature review showed that the modified poly (vinyl alcohol) (PVA) nanofiber by triethylenetetramine (TETA) was not used to remove dye from colored wastewater. In this paper, PVA–TETA nanofiber was prepared and crosslinked using glutaraldehyde (GA). Dye removal ability of the modified nanofiber (PVA–TETA–GA) from colored wastewater was studied. Fourier transform infrared spectroscopy (FTIR) and scanning electron microscopy (SEM) were used to investigate the characteristics of the modified nanofiber. The effect of operational parameters (adsorbent dosage, pH, and the initial dye concentration) on dye removal was studied. The dye adsorption isotherm and kinetics was studied.

2. Experimental

2.1. Chemicals

Poly(vinyl alcohol) (M_v = 145,000 g/mol) was purchased from Sigma (USA). Triethylenetetramine (TETA), glutaraldehyde, hydrochloric acid, sodium hydroxide, and acetic acid were obtained from Merck. Double-distilled water was used for the synthesis of nanofiber. Direct Red 80 (DR80), Direct Red 81 (DR81), and Reactive Red 180 (RR180) were used. The characteristics and chemical structures of the dyes are shown in Table 1 and Fig. 1, respectively.

2.2. Preparation of PVA-TETA-GA nanofiber

For the preparation of PVA–TETA $[CH_2NHCH_2CH_2NH_2]_2$, 7 wt% PVA solution was provided by dissolving 0.7 g of PVA in 10 mL deionized water. Then, different amounts of TETA (5, 2.5, 1.5, and 0.5 wt% of TETA) were added to PVA solution and sonicated for 3 h at 90˚C. Next, the prepared solutions were poured into 10-mL plastic syringe with a 0.5-mm-diameter capillary tip. A variable high-voltage generator was used for the electrospinning process. The positive terminal of a high-voltage generator was connected to the metallic syringe tip while the negative terminal was connected to an aluminum foil. The applied voltage was 21 kV. The electrospun fibers were collected on an aluminum foil coiled on a metal cylinder rotating at 200 rpm. The distance between the tip and the collector was 15 cm and the flow rate of the spinning solution was 1 mL/h. The fibers were crosslinked in glutaraldehyde vapor at 70˚C for 12 h, and heated at 70˚C for another 10 h to remove residual glutaraldehyde.

2.3. Characterization

Fourier transform infrared spectrometer, Equinox 55, from Bruker (Germany), was used to analyze the chemical and/or physical interactions over the wave number range of 4,000–400 cm^{-1}. The surface morphologies of the aminated PVA nanofibers were studied using an SEM, VEGA-II form Tescan (USA).

2.4. Adsorption studies

Adsorption experiments were carried out by agitating 0.01 g of the aminated nanofiber as an adsorbent with 200 mL of DR80, DR81 and RR180 (20 mg/L). The pH of each solution was adjusted to the desired value using HCl or NaOH. Single-beam UV spectrophotometer (CE-CILCE2021) is used for dye concentration measurements.

The effect of adsorbent dosage (0.08–0.012 g) on the dye removal was investigated by contacting 200 mL of the dye solution with an initial dye concentration of 20 mg/L and pH 2.1 at room temperature (25˚C) for

Table 1
The characteristics of dyes

Name	Molecular structure	Molecular formula	Molecular weight	λ_{max}
Direct Red 80	Multi-Azo class	$C_{45}H_{26}N_{10}Na_6O_{21}S_6$	1,373.08	528
Direct Red 81	Double Azo class	$C_{29}H_{19}N_5Na_2O_8S_2$	675.6	510
Reactive Red 180	Single Azo class	$C_{29}H_{19}N_3Na_4O_{17}S_5$	933.76	542

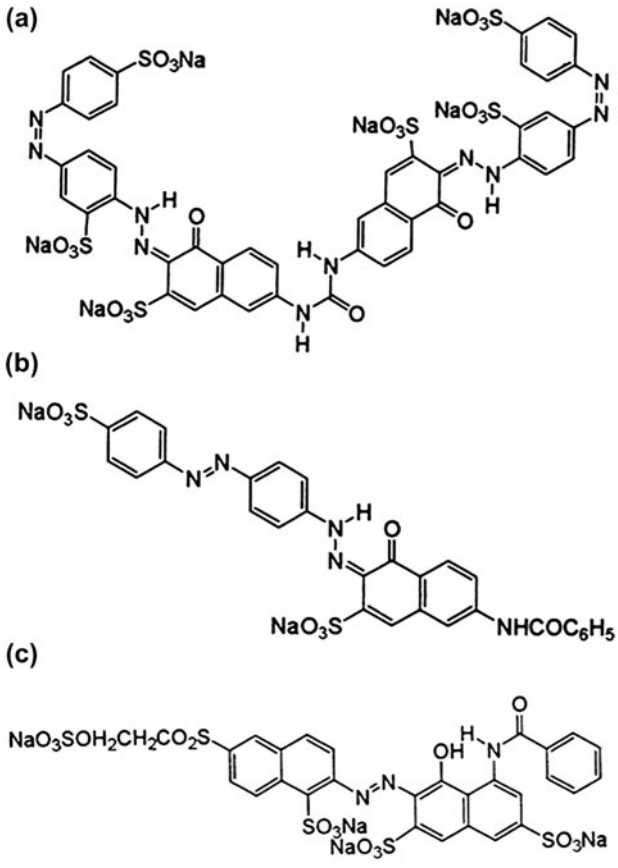

Fig. 1. The chemical structure (a) Direct red 80, (b) Direct red 81, and (c) Reactive Red 180.

1 h. The dye removal ability of nanofiber (0.011 g) at different pH values (2.1, 6, and 9) was studied by contacting 200 mL of the dye solution with an initial concentration (20 mg/L) at room temperature (25°C) for 1 h. The effect of the initial dye concentration (20, 30, 40, and 50 mg/L) on dye removal was investigated by contacting 200 mL of the dye solution with adsorbent (0.012 g) at pH 2.1 and room temperature (25°C) for 1 h.

3. Results and discussion

3.1. Reaction mechanism and characterization

The reactions of PVA, GA and TETA to prepare the modified nanofiber are shown in Fig. 2. Aldehyde reacts with alcohol to produce acetal [18]. In addition, aldehyde reacts with amine and the imine is synthesized [19,20]. Poly(vinyl alcohol) reacts with glutaraldehyde and triethylenetetramine to produce the modified nanofiber containing amine functional groups (Fig. 2).

FTIR spectrum of pure PVA is shown in Fig. 3(a). It shows that the major peaks of poly(vinyl alcohol) are C–H broad alkyl stretching bands ($v = 2{,}923$ and 2,851 cm^{-1}) and hydrogen-bonded band ($v = 3{,}432$ cm^{-1}). FTIR spectrum in Fig. 3(b) is associated with PVA and TETA crosslinked by glutaraldehyde (GA). It can be observed that two important peaks at $v = 2{,}860$ and 2,730 cm^{-1} of C–H stretching are related to aldehydes. By crosslinking PVA with GA (Fig. 3(b)), the O–H stretching vibration peak ($v = 3{,}444$ cm^{-1}) was decreased when compared to pure PVA (Fig. 3(a)). This result suggests that the hydrogen bonding becomes weaker in crosslinked PVA than in pure PVA because of the diminution in the number of OH groups and acetal formation (Fig. 3(a)). The relative increase in the C=O band at approximately $v = 1{,}730$ cm^{-1} indicates that the aldehyde groups of GA did not completely react with O–H groups of PVA chain and N–H groups of TETA. In addition, the C–O stretching at approximately 1,096 cm^{-1} in pure PVA is replaced by a broader absorption band (from $v = 1{,}000$ to 1,140 cm^{-1}), which can be attributed to the ether (C–O) and the acetal ring (C–O–C) bands formed by the crosslinking reaction of PVA with GA (Fig. 2). In addition, imine bands (–C=N–, 1,640–1,690 cm^{-1}) were formed by the crosslinking reaction of amine (TETA) with aldehyde (GA) (Fig. 2). Therefore, it can be assumed that GA has acted as a chemical crosslinker [18,20].

The SEM micrographs of PVA–TETA–GA nanofiber are shown in Fig. 4. The surface of the PVA–TETA–GA nanofiber exhibited similar morphologies compared to the PVA nanofibers mats, without any serious cracks or sign of degradation. In high conversions, adhesion among the nanofibers was found to decrease the effective surface area.

3.2. Adsorption studies

It has been well established that the solution pH has a significant effect on the adsorption process. The effect of the initial solution pH on dye removal for DR80, DR81, and RR180 is shown in Fig. 5. It is observed that the adsorption capacity increases when the pH decreases. The maximum adsorption of DR80, DR81, and RR180 occurred at pH 2.1. At this pH, a strong electrostatic attraction occurs between the positively charged nanofiber considering the ionization of functional groups (amine group, $-NH_3^+$) and the anionic dye molecules. The number of positively charged sites of PVA/TETA decreases at high pH values [21].

The effect of nanofiber dosage on the dye removal for DR80, DR81, and RR180 is shown in Fig. 6. The removal percentage increased with increasing nanofiber dosage up to a certain limit, then reached a

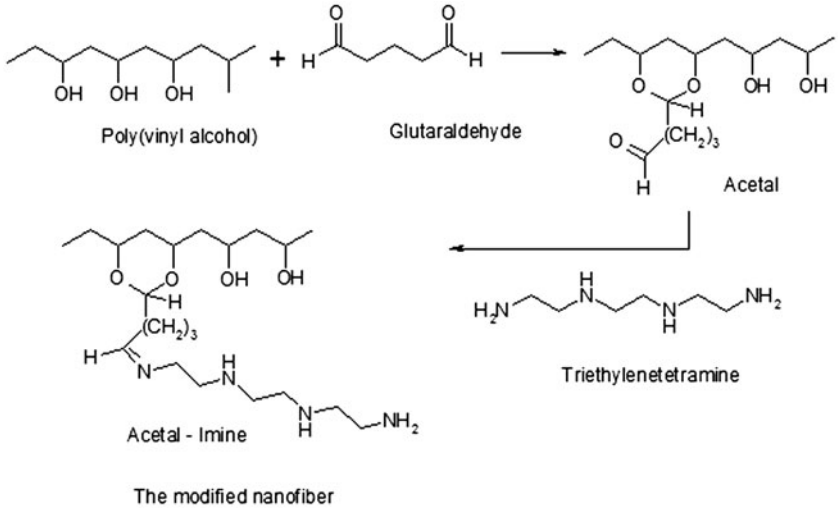

Fig. 2. The reactions of PVA, GA, and TETA to prepare the modified nanofiber (PVA-TETA-GA).

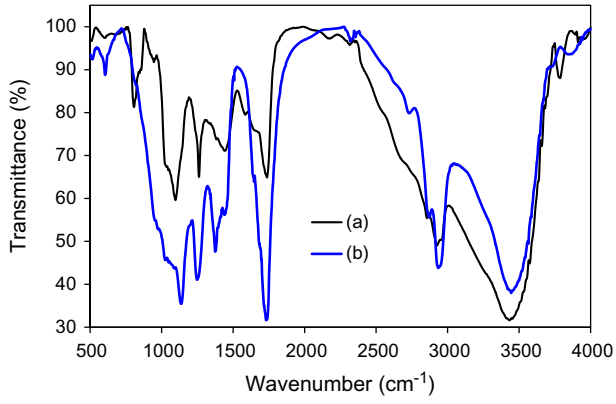

Fig. 3. FTIR spectrum of nanofibers (a) PVA and (b) PVA–TETA–GA.

constant value. The increasing dye removal with the adsorbent dosage can be attributed to increase in the adsorbent surface and availability of more adsorption sites on nanofiber [22–25].

The effect of initial dye concentration of DR80, DR81, and RR180 on dye removal is shown in Fig. 7. The results presented that dye removal decreases by increasing dye concentration because the active sites on adsorbent for dye removal decreases [25,26].

3.3. Adsorption isotherm

At equilibrium, an adsorption isotherm can be constructed as a relation of the adsorbate concentration at the surface and in the solution at a given constant temperature. Isotherm data should accurately fit into different isotherm models, to produce a suitable model for additional process studies [27]. The Langmuir, Freundlich, and Temkin isotherms were applied to the obtained results. The Langmuir equation is as follows:

$$\frac{C_e}{q_e} = \frac{1}{K_L Q_0} + \frac{C_e}{Q_0} \quad (1)$$

where q_e, C_e, K_L, and Q_0 are the amount of dye adsorbed on adsorbent at equilibrium (mg/g), the equilibrium concentration of dye solution (mg/L), Langmuir constant (L/g), and the maximum adsorption capacity (mg/g), respectively. To study the applicability of the Langmuir isotherm for dye adsorption onto adsorbent, a linear plot of C_e/q_e against C_e was plotted.

Also, isotherm data were tested with Freundlich isotherm that can be expressed by [27–29]:

$$\log q_e = \log K_F + (1/n) \log C_e \quad (2)$$

where K_F is the Freundlich constant and $1/n$ is the adsorption intensity [28,29].

The Temkin isotherm is given as follows:

$$q_e = B_1 \ln K_T + B_1 \ln C_e \quad (3)$$

where B_1 (RT/b) and K_T are the Temkin constants and can be determined by a plot of q_e vs. $\ln C_e$. Also, T is the absolute temperature (K) and R is the universal gas constant (8.314 J/mol K). The constant b is related to

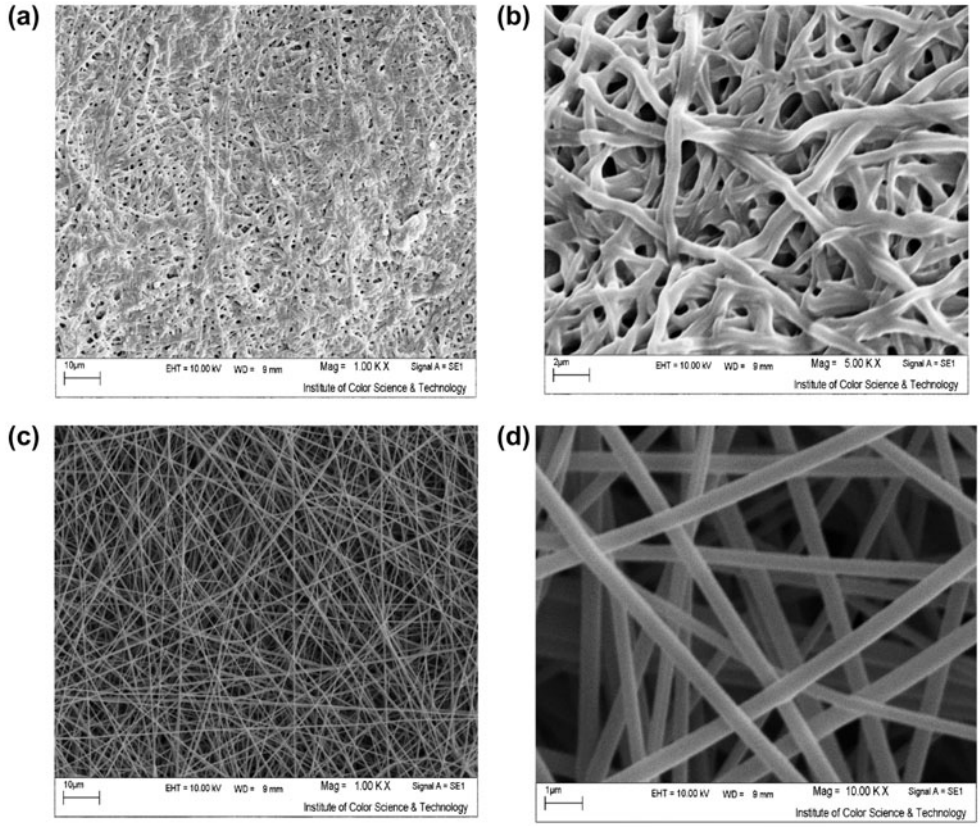

Fig. 4. SEM micrographs of PVA–TETA–GA nanofibers with 1.5 wt% of TETA (a and b) and 0.5 wt% of TETA (c and d).

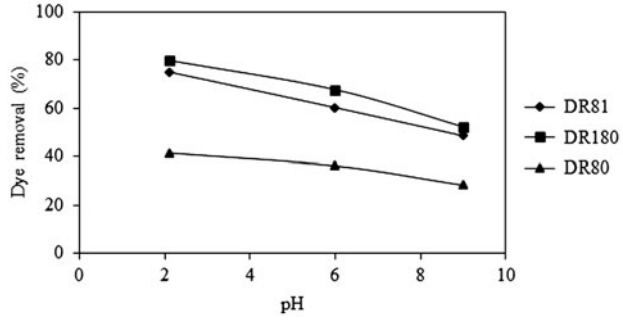

Fig. 5. The effect of solution pH on the adsorption of dyes by PVA–TETA–GA nanofiber (t: 60 min, C_0: 20 mg/L, m: 0.011 g).

the heat of adsorption. The Temkin isotherm assumes that the heat of adsorption of all the molecules in the layer decreases linearly with coverage due to adsorbent–adsorbate interactions. In addition, the adsorption is characterized by uniform distribution of binding energies, up to some maximum binding energy [30].

The values of Q_0, K_L, K_F, $1/n$, K_T, B_1, and R^2 (correlation coefficient values of all isotherms models) are shown in Table 2.

The Langmuir model yielded the best fit with the highest R^2 value of 0.99, thus the Langmuir isotherm was the most suitable equation to describe the adsorption equilibrium of dye on the PVA-TETA-GA nanofiber. The q_e values predicted from the Langmuir model agreed well with the experimental values. The results demonstrated the formation of monolayer coverage of dye molecule at the outer surface of the PVA–TETA–GA nanofiber.

3.4. Adsorption kinetics

Adsorption kinetics studies the adsorption mechanisms that are important for the efficiency of the process. At this point, characteristic constants of adsorption are determined using pseudo-first-order equation, pseudo-second-order equation, and intraparticle diffusion [31–34].

A linear form of pseudo-first-order model is:

$$\log(q_e - q_t) = \log(q_e) - \frac{k_1}{2.303}t \quad (4)$$

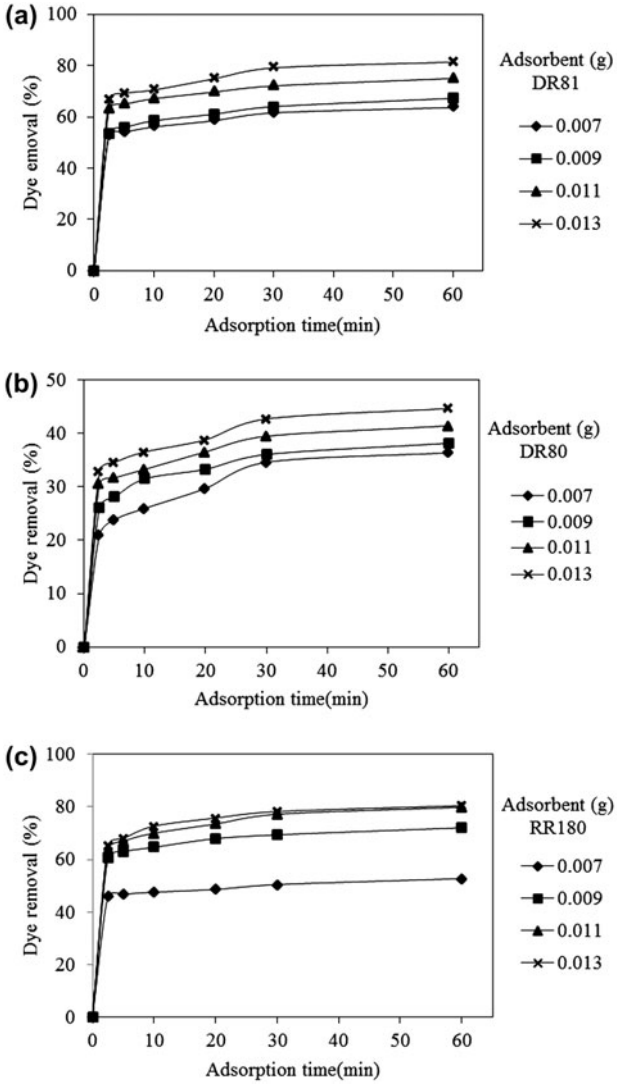

Fig. 6. The effect of nanofiber dosage on the adsorption of dyes (t: 60 min) (a) DR80, (b) DR81, and (c) RR180.

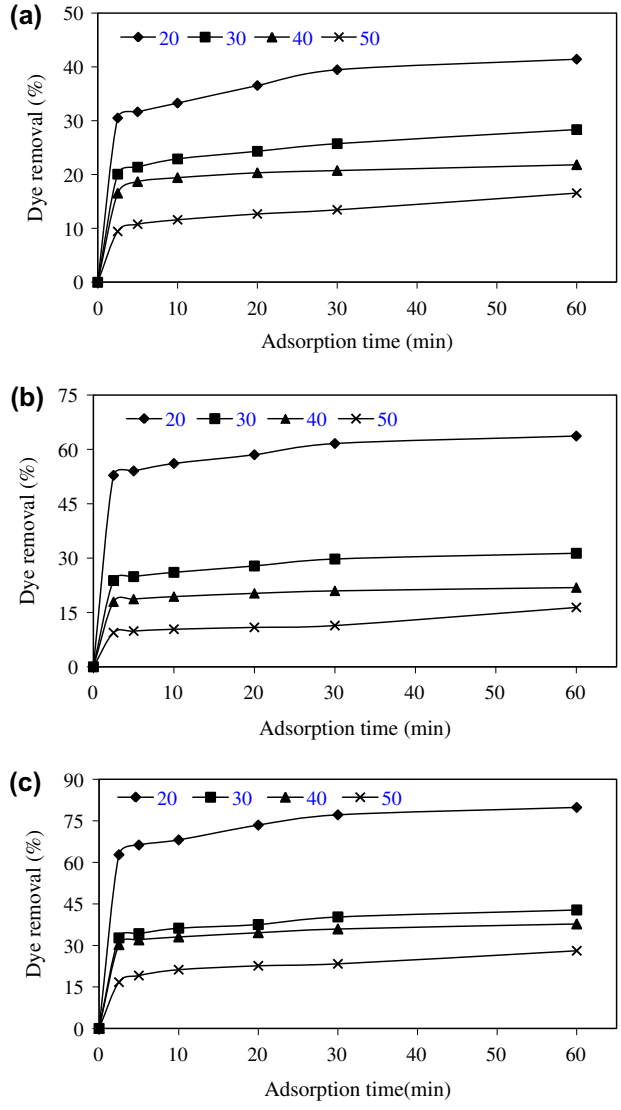

Fig. 7. The effect of initial dye concentration (mg/L) of DR80, DR81 and RR180 on the adsorption of dyes (t: 30 min) (a) DR80, (b) DR81, and (c) RR180.

where q_t, and k_1 are the amount of dye adsorbed at time t (mg/g), and the equilibrium rate constant of pseudo-first-order kinetics (1/min), respectively.

Linear form of pseudo-second-order model is illustrated as:

$$\frac{t}{q_t} = \frac{1}{k_2 q_e^2} + \frac{t}{q_e} \tag{5}$$

where k_2 is the equilibrium rate constant of pseudo-second-order (g/mg min).

The possibility of intraparticle diffusion resistance affecting adsorption is explored using the intra particle diffusion model as:

$$q_t = k_p t^{1/2} + I \tag{6}$$

where k_p and I are the intraparticle diffusion rate constant and intercept, respectively. To understand the applicability of the intraparticle diffusion, pseudo-second-order and pseudo-first-order, linear plots of q_t against $t^{1/2}$, t/q_t vs. t and $\log(q_e - q_t)$ vs. t at different dye concentrations (20, 30, 40, and 50 mg/L) are plotted, respectively. The kinetics constants for dye adsorption are shown in Table 3. The results illustrated that the rates of adsorption conform to the pseudo-second-order kinetics model. In addition, the experimental $q_e((q_e)_{Exp.})$ values are consistent with

Table 2
Isotherm constants for dye adsorption on nanofiber at different dye concentrations

	Isotherm								
	Langmuir			Freundlich			Temkin		
Dye	R^2	Q_0	K_L	R^2	$1/n$	K_F	R^2	B_1	K_T
DR80	0.999	128.205	19	0.056	0.542	134	0.547	19	134
DR81	0.999	178.570	56	0.234	0.019	147	0.229	56	147
RR180	0.999	181.818	83	0.709	0.009	198	0.707	83	197

Table 3
Kinetic constants for dye adsorption on nanofiber at different dye concentrations

			Pseudo-first-order			Pseudo-second-order			Intraparticle diffusion		
Dye (mg/L)		$(q_e)_{Exp.}$	R^2	$(q_e)_{Cal.}$	k_1	R^2	$(q_e)_{Cal.}$	k_2	R^2	I	k_p
DR80	20	115	0.9681	38	0.0697	0.9980	119	0.0039	0.9662	77	5
	30	118	0.9890	36	0.0398	0.9961	120	0.0034	0.9922	77	5
	40	120	0.9232	25	0.0525	0.9991	121	0.0064	0.8601	91	4
	50	118	0.9621	50	0.0281	0.9851	121	0.0018	0.9831	57	8
DR81	20	168	0.9631	35	0.0575	0.9992	169	0.0047	0.9720	132	5
	30	170	0.9750	48	0.0538	0.9983	175	0.0030	0.9784	120	7
	40	175	0.9964	34	0.0506	0.9942	178	0.0046	0.9731	138	5
	50	177	0.9674	74	0.0115	0.9454	181	0.0086	0.8493	77	11
RR180	20	176	0.9992	45	0.0640	0.9991	178	0.0039	0.9521	131	6
	30	177	0.9613	46	0.0461	0.9981	181	0.0029	0.9812	138	7
	40	179	0.9881	37	0.0481	0.9990	181	0.0041	0.9724	138	6
	50	181	0.8960	68	0.2902	0.9983	185	0.0014	0.9650	96	11

the calculated ones ($(q_e)_{Cal.}$) obtained from the linear plots of pseudo-second-order kinetics.

4. Conclusions

In this research, poly(vinyl alcohol) (PVA)–triethylenetetramine (TETA) nanofiber was prepared and crosslinked using glutaraldehyde (GA). Dye removal ability of the modified nanofiber (PVA–TETA–GA) from colored wastewater containing anionic dyes was studied. The characteristics of the modified nanofiber were investigated using FTIR and SEM. The effect of adsorbent dosage, pH, and the initial dye concentration on dye removal was studied. It is showed that the adsorption capacity increases when the pH decreases. Dye removal decreases as the dye concentration increases. The isotherm data confirm that the one-layer adsorption of dyes takes place at specific homogeneous sites of nanofiber surface (Langmuir model). The adsorption kinetics illustrated that the rates of dye adsorption on the modified nanofiber conform to the pseudo-second-order kinetics model.

References

[1] N.M. Mahmoodi, Zinc ferrite nanoparticle as a magnetic catalyst: Synthesis and dye degradation, Mater. Res. Bull. 48 (2013) 4255–4260.
[2] N.M. Mahmoodi, N.Y. Limaee, M. Arami, S. Borhany, M. Mohammad-Taheri, Nanophotocatalysis using nanoparticles of titania: Mineralization and finite element modelling of Solophenyl dye decolorization, J. Photochem. Photobiol., A: Chem. 189 (2007) 1–6.
[3] N.M. Mahmoodi, Photocatalytic ozonation of dyes using multiwalled carbon nanotube, J. Mol. Catal. A: Chem. 366 (2013) 254–260.
[4] S. Davarpanah, N.M. Mahmoodi, M. Arami, H. Bahrami, F. Mazaheri, Environmentally friendly surface modification of silk fiber: Chitosan grafting and dyeing, Appl. Surf. Sci. 255 (2009) 4171–4176.
[5] M. Ranjbar-Mohammadi, M. Arami, H. Bahrami, F. Mazaheri, N.M. Mahmoodi, Grafting of chitosan as a biopolymer onto wool fabric using anhydride bridge

and its antibacterial property, Colloid. Surf. B 76 (2010) 397–403.
[6] P.K. Neghlani, M. Rafizadeh, F.A. Taromi, Preparation of aminated-polyacrylonitrile nanofiber membranes for the adsorption of metal ions: Comparison with microfibers, J. Hazard. Mater. 186 (2011) 182–189.
[7] T. Pirzada, S.A. Arvidson, C.D. Saquing, S.S. Shah, S.A. Khan, Hybrid silica–PVA nanofibers via sol–gel electrospinning, Langmuir 28 (2012) 5834–5844.
[8] Y. Zhao, Y. Zhou, X. Wu, L. Wang, L. Xu, Sh. Wei, A facile method for electrospinning of Ag nanoparticles/poly(vinyl alcohol)/carboxymethyl - chitosan nanofibers, Appl. Surf. Sci. 258 (2012) 8867–8873.
[9] H. Wang, W. Wang, S. Jiang, Sh Jiang, Poly(vinyl alcohol)/oxidized starch fibres via electrospinning technique: Fabrication and characterization, Iran. Polym. J. 20 (2011) 551–558.
[10] R. Sharma, N. Singh, A. Gupta, S. Tiwari, S.K. Tiwari, S.R. Dhakate, Electrospun chitosan–polyvinyl alcohol composite nanofibers loaded with cerium for efficient removal of arsenic from contaminated water, J. Mater. Chem. A 2 (2014) 16669–16677.
[11] Z.G. Wang, L.S. Wan, Z.M. Liu, X.J. Huang, Z.K. Xu, Enzyme immobilization on electrospun polymer nanofibers: An overview, J. Mol. Catal. B: Enzym. 56 (2009) 189–195.
[12] Y. Wang, Y.L. Hsieh, Immobilization of lipase enzyme in polyvinyl alcohol (PVA) nanofibrous membranes, J. Membr. Sci. 309 (2008) 73–81.
[13] D. He, B. Hu, Q.F. Yao, K. Wang, S.H. Yu, Large-scale synthesis of flexible free-standing SERS substrates with high sensitivity: Electrospun PVA nanofibers embedded with controlled alignment of silver nanoparticles, ACS Nano 3 (2009) 3993–4002.
[14] Q. Gao, J. Luo, X. Wang, C. Gao, M. Ge, Novel hollow α-Fe_2O_3 nanofibers via electrospinning for dye adsorption, Nanoscale Res. Lett. 10 (2015) 176.
[15] E. Ghasemi, H. Ziyadi, A.M. Afshar, M. Sillanpää, Iron oxide nanofibers: A new magnetic catalyst for azo dyes degradation in aqueous solution, Chem. Eng. J. 264 (2015) 146–151.
[16] J. Yan, Y. Huang, Y.E. Miao, W.W. Tjiu, T. Liu, Polydopamine-coated electrospun poly(vinyl alcohol)/poly (acrylic acid) membranes as efficient dye adsorbent with good recyclability, J. Hazard. Mater. 283 (2015) 730–739.
[17] H. Hallaji, A.R. Keshtkar, M.A. Moosavian, A novel electrospun PVA/ZnO nanofiber adsorbent for U(VI), Cu(II) and Ni(II) removal from aqueous solution, J. Taiwan Inst. Chem. Eng 46 (2015) 109–118.
[18] E.F. Reis, F.S. Campos, A.P. Lage, R.C. Leite, L.G. Heneine, W.L. Vasconcelos, Z.I.P. Lobato, H.S. Mansur, Synthesis and characterization of poly(vinyl alcohol) hydrogels and hybrids for rMPB70 protein adsorption, Mater. Res. 9 (2006) 185–191.
[19] K. Mohajershojaei, N.M. Mahmoodi, A. Khosravi, Immobilization of laccase enzyme onto titania nanoparticle and decolorization of dyes from single and binary systems, Biotechnol. Bioprocess Eng. 20 (2015) 109–116.
[20] D.L. Pavia, G.M. Lampman, G.S. Kaiz, Introduction to Spectroscopy: A Guide for Students of Organic Chemistry, W.B. Saunders Company, Philadelphia, PA, 1987.
[21] N.M. Mahmoodi, Dendrimer functionalized nanoarchitecture: Synthesis and binary system dye removal, J. Taiwan Inst. Chem. Eng. 45 (2014) 20–45.
[22] N.M. Mahmoodi, Synthesis of amine-functionalized magnetic ferrite nanoparticle and its dye removal ability, J. Environ. Eng. 139 (2013) 1382–1390.
[23] N.M. Mahmoodi, S. Khorramfar, F. Najafi, Amine-functionalized silica nanoparticle: Preparation, characterizationand anionic dye removal ability, Desalination 279 (2011) 61–68.
[24] N.M. Mahmoodi, B. Hayati, M. Arami, H. Bahrami, Preparation, characterization and dye adsorption properties of biocompatible composite (alginate/titania nanoparticle), Desalination 275 (2011) 93–101.
[25] Z. Hosseinabadi-Farahani, N.M. Mahmoodi, H. Hosseini-Monfared, Preparation of surface functionalized graphene oxide nanosheet and its multicomponent dye removal ability from wastewater, Fibers Polym. 16 (2015) 1035–1047.
[26] S. Mali, C.S. Shim, H. Kim, J.V. Patil, D.H. Ahn, P.S. Patil, Ch.K. Hong, Evaluation of various diameters of titanium oxide nanofibers for efficient dye sensitized solar cells synthesized by electrospinning technique: A systematic study and their application, Electrochim. Acta 166 (2015) 356–366.
[27] N.M. Mahmoodi, Surface modification of magnetic nanoparticle and dye removal from ternary systems, J. Ind. Eng. Chem. 27 (2015) 251–259.
[28] K.Y. Foo, B.H. Hameed, Insights into the modeling of adsorption isotherm systems, Chem. Eng. J. 156 (2010) 2–10.
[29] M. Gouamid, M.R. Ouahrani, M.B. Bensaci, Adsorption equilibrium, kinetics and thermodynamics of Methylene Blue from aqueous solutions using date palm leaves, Energy Proc. 36 (2013) 898–907.
[30] M. Barkat, D. Nibou, S. Amokrane, S. Chegrouche, A. Mellah, Uranium(VI) adsorption on synthesized 4A and P1 zeolites: Equilibrium, kinetic, and thermodynamic studies, C.R. Chim. 18 (2015) 261–269.
[31] N.M. Mahmoodi, B. Hayati, M. Arami, Kinetic, equilibrium and thermodynamic studies of ternary system dye removal using a biopolymer, Ind. Crop. Prod. 35 (2009) 295–301.
[32] A. Haji, N.M. Mahmoodi, Soy meal hull activated carbon: Preparation, characterization and dye adsorption properties, Desalin. Water Treat. 44 (2012) 237–244.
[33] N.M. Mahmoodi, B. Hayati, H. Bahrami, M. Arami, Dye adsorption and desorption properties of Mentha pulegium in single and binary systems, J. Appl. Polym. Sci. 122 (2011) 1489–1499.
[34] B. Hayati, N.M. Mahmoodi, M. Arami, F. Mazaheri, Dye removal from colored textile wastewater by poly (propylene imine) dendrimer: Operational parameters and isotherm studies, Clean–Soil Air Water 39 (2011) 673–679.